1986MNRAS.219..903C

Mon. Not. R. astr. Soc. (1986) **219**, 903–926

The variation of interstellar extinction in the ultraviolet

David J. Carnochan *Department of Physics and Astronomy, University College London, Gower Street, London WC1E 6BT*

Accepted 1985 November 25. Received 1985 November 25; in original form 1985 July 1

Summary. One hundred and fifty-four reddened stars that are apparently normal in the visible were selected from the S2/68 Ultraviolet Sky Survey. The ultraviolet data for 92 of these cannot be explained in terms of a fixed interstellar extinction law. Between 1400 and 2740 Å the extinction curve for each star can be well represented by two parts; a straight-line scattering component and a Lorentzian 2200 Å absorption feature. Independent variations are found in both parts and these cannot be explained by photometric or spectral classification errors. Both parts vary smoothly implying that there is no fixed extinction law, and one star in three is found to depart from the mean law by more than 1 mag at either 1500 or 2200 Å. The two variations allow not only all 154 stars to be explained but also anomalous stars reported by other authors. These are not special but merely situated towards the limits of the variations. A variation in the relative proportions of graphite and silicate grains goes some way towards explaining the observations. The profile of the 2200 Å feature is determined, the symmetrical shape is confirmed, and the profile fits a Lorentzian very closely.

1 Introduction

The current situation regarding variations in the shape of the interstellar extinction curve is somewhat confusing. On the one hand several authors have produced mean extinction curves based on hundreds of stars. With the exception of a few individual stars, they have found no significant variations and have concluded that the general interstellar extinction law does follow a fixed curve (Nandy *et al.* 1975, 1976; Carnochan 1982). On the other hand many individual objects have been found where the extinction curves show large departures from the mean law both in the slope of the scattering continuum (e.g. Witt, Bohlin & Stecher 1984) and in the strength of the 2200 Å feature (e.g. Willis & Wilson 1975, 1977). And some authors have warned that variations are so common that the adoption of a mean extinction curve for the correction of interstellar reddening is dangerous and can lead to large errors (e.g. Massa, Savage & Fitzpatrick 1983). In all about 100 stars with anomalous extinction curves have been reported. It is not clear whether these anomalous curves are individually unique or form part of a more general variation, whether the anomalies are circumstellar or interstellar, and if circumstellar whether the

© Royal Astronomical Society • Provided by the NASA Astrophysics Data System

1986MNRAS.219..903C

anomalies arise from the stars being peculiar. Outside of our Galaxy it is now known that the extinction curves for the LMC (Nandy *et al.* 1981) and SMC (Bromage & Nandy 1983) are substantially different from the mean galactic law with the scattering component considerably steeper and with the 2200 Å feature much weaker or even absent.

This paper attempts to clarify the situation by studying a homogeneous sample of 154 normal stars taken from the S2/68 Ultraviolet Sky Survey. Section 2 describes the data and shows some anomalous extinction curves. Section 3 examines the variations by splitting the extinction curve into two components, a straight line law for the scattering continuum and a Lorentzian profile for the 2200 Å absorption feature. Section 4 shows that the variations are real and cannot be explained in terms of observational error or systematic effects. In Section 5 the profile of the 2200 Å feature is derived, without assuming the shape of the underlying scattering continuum. Section 6 examines the anomalous stars reported by other authors in terms of the parameters used in this paper. Section 7 looks at the expected variation in the extinction curve resulting from changes in the relative proportions of graphite and silicate grains. Section 8 examines the galactic distribution of the variations and Section 9 addresses the problem of reddening corrections.

2 Data reduction

The S2/68 Ultraviolet Sky Survey Telescope scanned the whole sky and measured the absolute fluxes for about 58 000 stars. These observations can provide the basis for many research programmes and in this paper they are used for a study of interstellar extinction. The form of the data has been described by Carnochan (1982) and essentially comprises 12 narrow band fluxes (full width 100 Å) centred every 100 Å between 1400 and 2500 Å, and a broad band flux (full width 330 Å) centred on 2740 Å. Stars were selected using the following criteria:

(i) An MK spectral type in the range B0 to B5 and luminosity class III to V. In establishing the intrinsic colours (Carnochan 1982) it was found that the O stars showed a large intrinsic scatter. This may be related to their emission lines or mass loss, or to the fact that very few O stars are unreddened which, for a variable extinction curve, will lead to an apparently large intrinsic scatter. Supergiants can give rise to large errors in the extinction curve, see Section 4, and their relatively low population means that the intrinsic colours are not as well determined as for luminosity classes III to V. Hence the decision to deliberately exclude O stars and luminosity classes Ia to II–III from this study.

(ii) *UBV* photometry and a derived $E(B-V)>0.20$, i.e. little reddened stars were excluded.

(iii) No emission lines or peculiarities, i.e. all *e* and *p* stars were excluded.

(iv) The MK spectral type agreed with the *UBV* photometry. $(B-V)_0$ and $E(B-V)$ were derived using (a) MK type and a $(B-V)$ and (b) luminosity class and *UBV*, via the $Q=(U-B)-0.72(B-V)$ parameter. Only stars where both values of $(B-V)_0$ and $E(B-V)$ agreed to 0.025 or better were selected.

(v) Good quality S2/68 data, i.e. faint stars, stars with noisy data, and stars partially blended with nearby objects were excluded.

These selection criteria resulted in a set of 154 reddened stars with well defined MK spectral type and reddening $E(B-V)$, and apparently normal in the visible part of the spectrum. It is to be noted that this sample is (a) complete, in the sense that all 58 000 stars in the S2/68 survey were examined, and (b) unbiased, in the sense that no attempt was made to select stars on the basis of peculiar extinction. The stars are listed in Table 1.

If each star is normal then its observed ultraviolet colours, $[m(\lambda)-V]$, can be reproduced by taking the intrinsic colours, $[m(\lambda)-V]_0$, for the same MK type and reddening them by the observed colour excess, $E(B-V)$, using the mean interstellar extinction law. If the observed

© Royal Astronomical Society • Provided by the NASA Astrophysics Data System

1986MNRAS.219..903C

Table 1. Selected stars. One hundred and fifty-four normal reddened stars selected from the S2/68 ultraviolet sky survey. HD numbers marked with an asterisk cannot be explained by a fixed reddening law. A, B, sA, sB are the intercept, slope and errors for the linear scattering part of the star's individual extinction curve (normalized to 3.20 at V and 6.24 at 2740 Å). Very steep, steep, shallow or very shallow lines are marked by ++, +, − or −− respectively. G and sG are the magnitude and error of the Lorentzian fit to the 2200 Å feature, Very strong, strong, weak or very weak 2200 Å are marked by ++, +, − or −− respectively.

HD	MK Type	V	B-V	U-B	E(B-V)	A	sA	B	sB		G	sG	
593*	B 1 V	6.70	0.02	-0.75	0.28	3.4	.2	0.45	.03	−	4.4	.1	+
1544	B 0 III	8.12	0.16	-0.76	0.46	2.3	.2	0.88	.04		2.9	.2	−
2329*	B 3 V	7.43	0.07	-0.52	0.27	2.7	.2	0.74	.03		3.7	.1	
2451	B 0.5IV	8.74	0.19	-0.73	0.47	1.2	.3	1.09	.04	+	4.0	.2	
2654	B 2 V	7.39	-0.02	-0.69	0.22	2.8	.2	0.60	.04	−	5.0	.1	++
3950*	B 1 III	6.91	0.12	-0.68	0.38	1.7	.2	1.05	.03	+	2.5	.1	−−
7252	B 1 V	7.13	0.08	-0.74	0.34	1.4	.3	1.04	.04	+	4.3	.2	+
8965	B 0.5V	7.28	0.02	-0.82	0.30	1.5	.2	0.96	.04	+	4.6	.1	+
12709*	B 4 IV	7.95	0.09	-0.47	0.27	1.6	.3	0.97	.04	+	3.6	.2	
12740*	B 1 V	7.94	-0.05	-0.82	0.21	0.2	.3	1.49	.04	++	2.2	.2	−−
18352	B 1 V	6.82	0.21	-0.65	0.47	2.1	.2	0.85	.02		4.0	.1	
21483*	B 3 III	7.04	0.35	-0.33	0.55	1.9	.2	1.01	.03	+	2.5	.1	−−
21803	B 2 IV	6.41	0.03	-0.72	0.27	0.9	.2	1.15	.03	+	4.7	.1	+
21856	B 1 V	5.89	-0.07	-0.85	0.19	1.9	.3	0.85	.04		4.8	.1	+
22253	B 0.5III	6.53	0.34	-0.56	0.62	1.9	.2	0.95	.03	+	3.6	.1	
22951*	B 0.5V	4.97	-0.02	-0.82	0.26	3.3	.2	0.54	.03	−	4.1	.1	
23180*	B 1 III	3.83	0.05	-0.75	0.31	2.7	.2	0.75	.03		3.4	.1	
23625*	B 2.5V	6.55	0.07	-0.61	0.29	3.7	.2	0.38	.03	−−	4.7	.1	+
23800*	B 1 IV	6.94	0.32	-0.54	0.58	2.5	.2	0.89	.03		2.7	.1	−
24131*	B 1 V	5.76	0.01	-0.80	0.27	3.6	.2	0.39	.03	−−	5.1	.1	++
24190*	B 2 V	7.43	0.04	-0.63	0.28	3.6	.2	0.46	.03	−	3.9	.1	
24640*	B 1.5V	5.48	-0.03	-0.75	0.22	3.6	.2	0.41	.03	−	4.8	.1	+
25787	B 2 V	7.65	0.02	-0.75	0.26	0.8	.2	1.14	.03	+	5.2	.1	++
27192*	B 2 IV	5.55	-0.01	-0.76	0.23	2.2	.2	0.74	.03		5.6	.1	++
27778*	B 3 V	6.34	0.20	-0.37	0.40	2.4	.2	0.90	.03		2.1	.1	−−
28446*	B 0 III	5.77	0.16	-0.73	0.46	1.7	.2	0.93	.04		4.5	.1	+
31894	B 2 IV	8.41	0.04	-0.66	0.28	3.8	.2	0.54	.04	−	2.1	.2	−−
32672*	B 2 IV-V	7.75	0.17	-0.54	0.41	3.1	.2	0.59	.03	−	4.1	.1	
32989	B 2 IV	8.04	0.06	-0.63	0.30	2.7	.2	0.76	.03		3.4	.1	
32990*	B 2 V	5.50	0.06	-0.56	0.30	2.6	.1	0.73	.02		3.9	.1	
35215	B 1 V	9.40	0.08	-0.66	0.34	4.8	.2	0.25	.04	−−	2.5	.2	−−
35633*	B 0.5IV	8.04	0.32	-0.66	0.60	3.2	.2	0.62	.03	−	2.8	.2	−
35653	B 0.5V	7.44	0.12	-0.75	0.40	1.4	.2	1.07	.03	+	4.0	.1	
36441*	B 1 V	8.25	0.06	-0.77	0.32	3.2	.2	0.47	.03	−	4.7	.1	+
36629*	B 2 V	7.65	0.02	-0.66	0.26	3.4	.2	0.42	.03	−	4.6	.1	+
37356*	B 2 IV-V	6.19	-0.04	-0.72	0.20	3.1	.2	0.56	.03	−	4.4	.1	+
37367*	B 2 V	5.95	0.16	-0.51	0.40	2.7	.1	0.66	.02	−	4.5	.1	+
37903*	B 1.5V	7.82	0.10	-0.62	0.35	3.6	.2	0.42	.04	−	3.5	.1	
41690*	B 1 V	7.71	0.21	-0.61	0.47	0.6	.2	1.30	.03	++	3.7	.1	
42352*	B 1 III	6.93	-0.01	-0.80	0.25	3.0	.2	0.62	.03	−	3.5	.1	
42745	B 2 V	8.11	0.03	-0.59	0.27	3.6	.2	0.51	.03	−	3.0	.1	−
42896	B 1 V	8.59	-0.07	-0.86	0.19	1.1	.2	1.10	.04	+	4.6	.1	+
47417	B 0 IV	6.97	0.01	-0.86	0.31	1.4	.2	1.04	.03	+	4.0	.1	
51756*	B 0.5IV	7.23	-0.07	-0.91	0.21	2.4	.2	0.73	.04		4.5	.1	+
52559*	B 2 IV-V	6.58	-0.02	-0.64	0.22	-0.2	.2	1.63	.03	++	1.9	.1	−−

© Royal Astronomical Society • Provided by the NASA Astrophysics Data System

1986MNRAS.219..903C

Table 1 – *continued*

HD	MK Type	V	B-V	U-B	E(B-V)	A	sA	B	sB	G	sG	
53456	B 0 V	7.22	0.00	-0.81	0.30	1.7	.2	0.96	.03 +	4.0	.1	
53755*	B 0.5V	6.48	-0.05	-0.89	0.23	0.2	.2	1.43	.03 ++	3.7	.1	
53974	B 0.5III	5.38	0.04	-0.85	0.32	1.5	.2	1.04	.03 +	3.9	.1	
54439	B 2 III	7.69	0.04	-0.76	0.28	2.8	.2	0.60	.04 -	4.8	.2	+
60196	B 0.5III	8.97	0.02	-0.86	0.30	2.3	.2	0.89	.04	3.1	.2	-
68761	B 0.5III-IV	6.54	-0.07	-0.92	0.21	2.4	.2	0.82	.04	3.2	.1	-
69882	B 1 III	7.15	0.35	-0.51	0.61	2.1	.2	0.92	.03	3.6	.1	
76838*	B 1 V	7.31	0.00	-0.72	0.26	2.9	.3	0.71	.05	3.5	.2	
91272	B 4 IV	6.18	0.01	-0.53	0.19	2.7	.2	0.66	.04 -	4.3	.1	+
92936*	B 2 III	7.04	-0.04	-0.82	0.20	-1.1	.3	1.76	.05 ++	3.4	.2	-
93714*	B 3 III	6.54	0.03	-0.60	0.23	3.3	.3	0.53	.04 -	4.1	.2	
97969	B 1 V	7.71	0.00	-0.76	0.26	3.2	.3	0.68	.05	2.2	.2	--
98695*	B 4 V	6.40	0.05	-0.48	0.23	4.9	.3	0.20	.04 --	3.3	.2	-
99264*	B 2 IV-V	5.58	0.06	-0.58	0.30	3.9	.2	0.40	.03 -	3.7	.1	
99872*	B 3 V	6.08	0.16	-0.43	0.36	3.5	.2	0.49	.03 -	4.0	.1	
99890*	B 0.5V	8.32	-0.06	-0.93	0.22	-1.1	.3	1.87	.05 ++	2.7	.2	-
102101*	B 2.5III	7.62	0.08	-0.65	0.30	-0.1	.3	1.43	.04 ++	4.4	.2	+
105139*	B 3 III	7.56	0.02	-0.65	0.22	2.5	.3	0.51	.05 -	6.7	.2	++
142096*	B 2.5V	5.02	-0.01	-0.58	0.21	3.9	.2	0.43	.03 -	3.3	.1	-
144470*	B 1 V	3.96	-0.04	-0.82	0.22	2.7	.2	0.61	.03 -	5.1	.1	++
145502*	B 2 IV	4.01	0.03	-0.64	0.27	4.3	.2	0.25	.04 --	4.2	.1	
147165*	B 1 III	2.87	0.14	-0.70	0.40	4.3	.2	0.27	.03 --	3.7	.1	
147933*	B 2 IV	4.61	0.23	-0.56	0.47	3.7	.2	0.38	.03 --	5.0	.1	++
149363	B 0.5III	7.80	0.03	-0.82	0.31	1.8	.2	0.87	.04	4.6	.1	+
149711*	B 2.5IV	5.83	-0.02	-0.61	0.20	3.5	.2	0.49	.03 -	3.8	.1	
151213	B 0 IV	7.64	0.29	-0.64	0.59	1.7	.2	0.88	.04	5.0	.2	++
154445*	B 1 V	5.63	0.16	-0.66	0.42	3.4	.1	0.47	.02 -	4.7	.1	+
155217	B 1 V	8.64	0.01	-0.74	0.27	3.2	.2	0.56	.04 -	3.7	.2	
155320	B 0.5V	8.35	0.09	-0.71	0.37	2.9	.2	0.69	.03	3.4	.1	-
155851*	B 0 V	8.19	0.13	-0.72	0.43	2.7	.2	0.79	.03	2.8	.1	-
156575*	B 1.5III	7.34	0.22	-0.65	0.47	2.5	.2	0.81	.04	3.4	.2	-
158186*	B 0 V	6.99	0.03	-0.86	0.33	2.6	.2	0.73	.03	4.0	.1	
159090*	B 0 III	7.40	0.16	-0.77	0.46	2.5	.2	0.76	.03	3.8	.1	
161056*	B 1.5V	6.30	0.38	-0.50	0.63	2.4	.1	0.79	.02	3.7	.1	
161756*	B 3 IV	6.35	0.12	-0.44	0.32	3.0	.2	0.63	.03 -	3.7	.1	
161961	B 0.5III	7.89	0.23	-0.67	0.51	1.8	.2	0.93	.03	4.3	.1	+
163472*	B 2 IV-V	5.82	0.09	-0.66	0.33	2.5	.1	0.71	.02	4.7	.1	+
164002	B 0.5V	7.42	0.00	-0.79	0.28	2.8	.2	0.64	.03 -	4.1	.1	
164581*	B 1 V	6.81	0.12	-0.66	0.38	2.3	.1	0.79	.02	4.3	.1	+
165016	B 0 III	7.33	-0.04	-0.86	0.26	2.9	.2	0.70	.04	3.7	.1	
165174*	B 0 III	6.13	-0.01	-0.92	0.29	1.6	.2	1.03	.03 +	4.0	.1	
166287*	B 0.5III	7.88	0.20	-0.66	0.48	2.7	.2	0.68	.03	3.9	.1	
166540	B 0.5IV	8.14	0.16	-0.73	0.44	2.2	.2	0.89	.03	3.1	.1	-
166803*	B 0.5III	8.17	0.12	-0.75	0.40	3.0	.2	0.57	.03 -	4.1	.1	
167088	B 0 V	8.54	0.02	-0.83	0.32	2.1	.3	0.79	.04	4.5	.2	+
170580*	B 2 V	6.66	0.11	-0.51	0.35	2.4	.1	0.83	.02	3.1	.1	-
170740*	B 2 V	5.72	0.24	-0.45	0.48	2.5	.1	0.79	.02	3.3	.1	-
170978*	B 3 IV	6.82	0.04	-0.48	0.24	3.1	.2	0.57	.03 -	3.9	.1	
172488*	B 0.5V	7.62	0.54	-0.40	0.82	1.7	.1	1.07	.02 +	2.6	.1	--
176254	B 2 IV	6.76	0.04	-0.56	0.28	2.8	.2	0.75	.03	3.3	.1	-
176304*	B 2 V	6.74	0.25	-0.44	0.49	1.9	.1	0.98	.02 +	3.2	.1	-
176819*	B 2 IV-V	6.68	0.02	-0.70	0.26	2.8	.2	0.64	.03 -	4.0	.1	
176853	B 2 V	6.65	0.21	-0.44	0.45	2.4	.1	0.80	.02	3.5	.1	
179406*	B 3 IV	5.34	0.13	-0.45	0.33	2.9	.1	0.67	.02	3.7	.1	
180968*	B 0.5IV	5.42	0.02	-0.80	0.30	1.9	.2	0.93	.03	3.7	.1	

© Royal Astronomical Society • Provided by the NASA Astrophysics Data System

1986MNRAS.219..903C

Table 1 – *continued*

HD	MK Type	V	B-V	U-B	E(B-V)	A	sA	B	sB	G	sG
181360*	B 3 V	7.60	0.05	-0.48	0.25	2.9	.2	0.65	.03 -	3.7	.1
181963	B 2 V	7.41	-0.04	-0.75	0.20	2.2	.4	0.70	.06	5.5	.2 ++
182032*	B 2.5V	7.43	-0.01	-0.56	0.21	3.9	.2	0.41	.04 -	3.5	.1
183013*	B 2 IV	7.39	0.09	-0.65	0.33	4.0	.2	0.33	.03 --	4.3	.1 +
184279*	B 0.5IV	6.93	0.03	-0.78	0.31	3.1	.2	0.65	.02 -	3.1	.1 -
184915*	B 0.5III	4.96	-0.01	-0.88	0.27	2.1	.2	0.84	.03	4.2	.1 +
185423*	B 3 III	6.35	0.04	-0.55	0.24	2.0	.2	0.90	.03	4.4	.1 +
185780*	B 0 III	7.74	-0.07	-0.92	0.23	0.2	.2	1.43	.04 ++	3.3	.1 -
186660*	B 3 III	6.47	0.05	-0.53	0.25	3.8	.2	0.42	.03 -	4.1	.1
187320	B 2 III	7.39	0.14	-0.64	0.38	1.4	.2	1.08	.03 +	3.9	.1
187851	B 2 V	7.74	0.13	-0.63	0.37	1.5	.2	1.04	.03 +	3.9	.1
188891	B 1 V	7.30	-0.01	-0.74	0.25	1.0	.2	1.18	.03 +	4.2	.1
189957	B 0 III	7.81	0.01	-0.86	0.31	1.8	.2	1.06	.03 +	2.5	.1 --
191456*	B 0.5III	7.45	0.04	-0.79	0.32	1.3	.2	1.11	.03 +	3.3	.1 -
191746	B 2 IV	7.17	0.01	-0.67	0.25	1.9	.2	0.99	.03 +	3.4	.1
192539	B 2 III	7.29	0.12	-0.64	0.36	1.7	.2	0.94	.03	4.6	.1 +
192575*	B 0.5V	6.82	0.15	-0.67	0.43	2.3	.1	0.87	.02	2.7	.1 -
193855	B 2 IV	7.78	0.27	-0.42	0.51	2.0	.2	0.94	.03	3.6	.1
194092*	B 0.5III	8.26	0.13	-0.74	0.41	3.1	.2	0.58	.04 -	4.5	.2 +
195089	B 2 IV	7.31	-0.02	-0.62	0.22	2.7	.2	0.77	.03	3.1	.1 -
195907	B 1.5V	7.82	0.03	-0.74	0.28	1.0	.2	1.13	.03 +	3.9	.1
195965*	B 0 V	6.98	-0.05	-0.90	0.25	1.1	.2	1.10	.04 +	4.7	.1 +
196421	B 2 IV	8.03	0.12	-0.63	0.36	1.6	.2	1.04	.04 +	3.0	.2 -
197770	B 2 III	6.32	0.33	-0.48	0.57	2.6	.2	0.76	.02	3.7	.1
198781*	B 0.5V	6.45	0.06	-0.77	0.34	0.8	.1	1.29	.02 ++	3.1	.1 -
201795*	B 1 V	7.53	-0.04	-0.85	0.22	1.3	.2	0.95	.04 +	6.2	.1 ++
202214*	B 0 V	5.64	0.11	-0.77	0.41	2.5	.2	0.76	.03	4.0	.1
202253	B 2 III	7.75	0.14	-0.61	0.38	3.4	.2	0.58	.04 -	3.0	.1 -
203532	B 5 V	6.38	0.13	-0.37	0.29	2.1	.2	0.93	.03	3.1	.1 -
204150	B 2 V	7.71	0.01	-0.76	0.25	1.4	.2	0.96	.03 +	4.6	.1 +
206183	B 0 V	7.42	0.14	-0.79	0.44	2.2	.2	0.88	.03	3.4	.1
206259	B 3 III	7.54	0.05	-0.57	0.25	2.1	.3	0.87	.04	3.2	.2 -
207538*	B 0 V	7.29	0.32	-0.64	0.62	1.8	.2	1.03	.03 +	3.0	.1 -
207793*	B 0.5III	6.60	0.38	-0.56	0.66	1.8	.2	0.99	.03 +	3.6	.1
208185*	B 2 V	7.38	0.11	-0.56	0.35	1.9	.2	0.95	.03 +	3.3	.1 -
209145*	B 1 V	7.62	0.33	-0.51	0.58	0.8	.2	1.11	.03 +	5.4	.2 ++
209339*	B 0 IV	6.65	0.07	-0.83	0.37	2.3	.2	0.80	.03	4.2	.1 +
209744*	B 1 V	6.70	0.22	-0.61	0.48	2.3	.2	0.88	.03	2.7	.1 -
211880*	B 0.5V	7.75	0.32	-0.61	0.60	1.7	.2	0.92	.03	4.3	.1 +
215371	B 1.5V	6.73	-0.02	-0.67	0.23	2.7	.2	0.74	.03	3.4	.1 -
216200*	B 3 IV	5.93	0.08	-0.50	0.28	1.3	.2	1.17	.03 +	2.8	.1 -
217035*	B 0 V	7.75	0.46	-0.53	0.76	2.9	.2	0.61	.03 -	3.9	.2
217297*	B 1 V	7.41	0.32	-0.56	0.58	2.9	.2	0.71	.03	3.4	.1 -
217811	B 2 V	6.39	-0.01	-0.58	0.23	2.4	.2	0.83	.03	3.2	.1 -
217943	B 2 V	6.73	-0.02	-0.64	0.22	2.8	.2	0.66	.04 -	3.8	.1
218342	B 0 IV	7.41	0.42	-0.54	0.71	2.3	.2	0.86	.03	3.2	.1 -
218376*	B 1 III	4.86	0.03	-0.87	0.29	1.3	.2	1.04	.04 +	4.8	.1 +
218440*	B 2 V	6.39	-0.01	-0.64	0.23	2.8	.2	0.65	.03 -	4.1	.1
218537*	B 2.5V	6.26	-0.02	-0.60	0.20	2.5	.2	0.72	.03	4.1	.1
218674	B 3 IV	6.78	0.01	-0.57	0.21	1.5	.2	1.05	.04 +	3.0	.1 -
219634	B 0 V	6.53	0.22	-0.67	0.52	2.3	.2	0.83	.03	3.7	.1
220562	B 2 V	6.79	0.25	-0.47	0.49	2.2	.2	0.81	.03	4.0	.1
224257	B 0 IV	7.99	-0.06	-0.90	0.24	1.9	.2	0.92	.04	3.5	.1
251847	B 1 IV	8.94	0.09	-0.78	0.35	3.5	.2	0.47	.04 -	2.8	.2 -

© Royal Astronomical Society • Provided by the NASA Astrophysics Data System

1986MNRAS.219..903C

colours cannot be reproduced then either the star or the extinction is anomalous. A star can only be shown to be anomalous by comparison with a normal star and to this end a complete grid of intrinsic colours was established together with a fresh determination of the mean interstellar extinction curve (Carnochan 1982). The majority of S2/68 stars can be fitted by selecting a star from the grid of intrinsic colours and applying a certain amount of reddening. Stars for which both an MK type and *UBV* photometry are available may at first sight appear anomalous if the cited MK type and derived $E(B-V)$ are used. However, these stars can usually be fitted by making slight adjustments to the MK type (up to 1 subclass) and reddening [up to 0.05 in $E(B-V)$].

One can attempt to fit the observed ultraviolet colours $[m(\lambda)-V]$, against a star of arbitrary spectral type by adjusting the amount of interstellar extinction, $E(B-V)$. The fit is acceptable if the external errors (i.e. the differences between the observed colours, $[m(\lambda)-V]$, and the reddened intrinsic colours) are comparable to the internal errors (as derived from the star's photometric errors and the errors of the intrinsic colours). A further constraint on the fit is that the observed differences should not show any systematic effects with wavelength. Fig. 1(a) illustrates this procedure for HD 217811 [B2V, $V=6.39$, $B-V=0.01$, $U-B=0.58$, $E(B-V)=0.21$]. The thick line is the mean external error, s, the thin line the mean internal error, σ, and the dashed line the extinction $E(B-V)$. It is clear that the external error agrees with the internal error at B2V and the actual best fit (working to fractional spectral classes) is: B2.3V, $V=6.36$, $B-V=0.03$, $U-B=0.57$, $E(B-V)=0.25$. Fig. 1(b) shows the observed colours, $[m(\lambda)-V]$, together with the expected colours for a B2V star with $E(B-V)=0.21$ (thick line), and the best fit colours (thin line). As mentioned above a satisfactory fit can be found for most stars by making slight adjustments to the cited MK spectral type and reddening.

Fig. 2(a) shows the fitting diagram for HD 37367, [B2V, $V=5.95$, $E(B-V)=0.40$], and it is clear that no acceptable fit can be found for any combination of spectral type and reddening. The best fit to this star is B0V, $V=5.94$, $E(B-V)=0.58$, for which the ratio of external to internal errors is 4.2. Apart from the discrepancy in the MK type (2 subclasses) and extinction [0.18 in

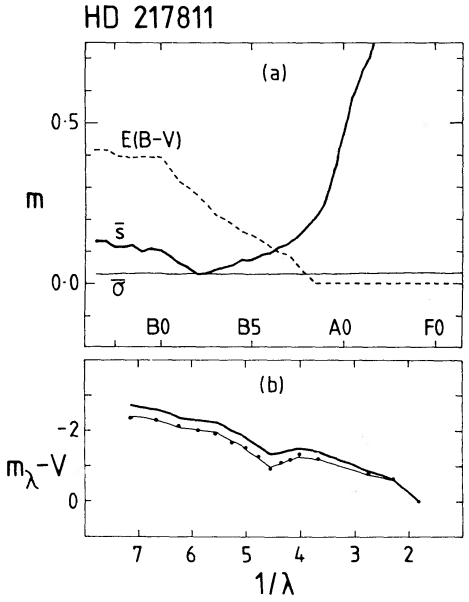


Figure 1. (a) The fit against class V spectral types for HD 217811. The thick line is the mean observed error, the thin line the mean expected error, and the dashed line the required extinction $E(B-V)$. The minimum observed error gives the best fit, in this case at B2.3V. (b) The S2/68 spectrum of HD 217811 plotted as $m(\lambda)-V$ against $1/\lambda$ in microns. The thick line indicates the expected ultraviolet colours based on the cited MK type and *UBV* photometry. The thin line through the data points is the best fit from Fig. 1(a).

© Royal Astronomical Society • Provided by the NASA Astrophysics Data System

1986MNRAS.219..903C

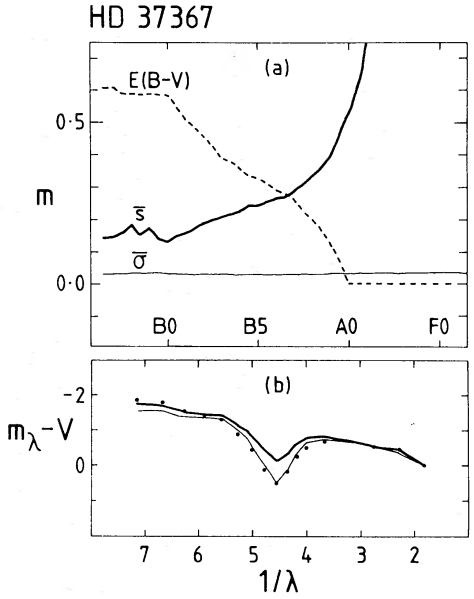


Figure 2. (a) The fit against class V spectral type for HD 37367. The thick line is the mean observed error, the thin line the mean expected error, and the dashed line the required extinction $E(B-V)$. At no point does the observed error approach the expected error indicating that no acceptable fit is possible. (b) The S2/68 spectrum for HD 37367 plotted as $m(\lambda)-V$ against $1/\lambda$ in microns. The thick line indicates the expected ultraviolet colours based on the cited MK type and *UBV* photometry. The thin line through the data points is the best fit from Fig. 2(a), for a B0V star.

$E(B-V)$], the fit departs systematically from the observed values shortwards of 1800 Å, see Fig. 2(b). The expected colours for this star, thick line, fit reasonably well in the visible and far-ultraviolet with the only area of discrepancy being that covered by the 2200 Å feature. This star appears to have a near normal scattering extinction but an excess 2200 Å absorption feature, and it is the excess 2200 Å feature that prevents an acceptable fit being found.

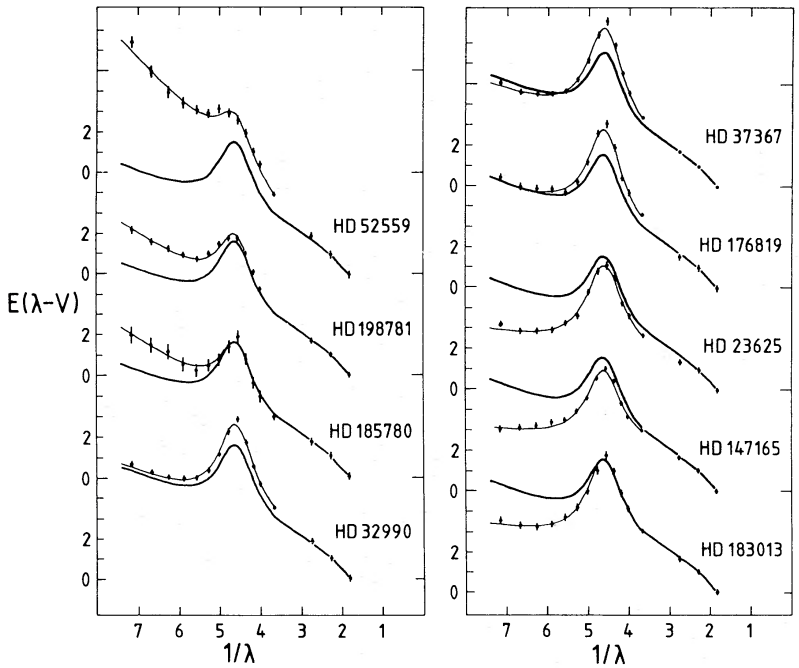


Figure 3. The normalized extinction curves for nine anomalous stars. For each star the thick line is the mean extinction curve and the thin line through the data points the best fit straight line and a Lorentzian.

© Royal Astronomical Society • Provided by the NASA Astrophysics Data System

1986MNRAS.219..903C

An examination of the 154 selected stars revealed that acceptable fits could not be found for 92 of the stars (i.e. mean external error>2.0×mean internal error). These stars are marked with an asterisk in Table 1. One of the selection criteria for the sample of stars was their apparent normality in the visible. Hence the most likely explanation for the inability to fit 92 out of 154 is that the interstellar extinction in the ultraviolet is anomalous. This is reinforced by the fact that, although spectral type mismatch is the dominant source of error in deriving extinction curves, these 92 stars could not be fitted against any spectral type. And again stars like HD 37367 where the only area of disagreement is around 2200 Å, the region occupied by the 2200 Å extinction feature, also point to the interstellar extinction law as being the source of the discrepancy.

Individual extinction curves were constructed for all of the stars based on their cited MK spectral type and *UBV* photometry. The extinction curve for each star was formed by differencing the star's observed colours $[m(\lambda)-V]$ with the intrinsic colours for the same MK spectral type (Carnochan 1982). The curve was then normalized to 3.20 at V and 4.20 at B [i.e. $E(B-V)=1.0$] using the cited *UBV* photometry. Fig. 3 shows the normalized extinction curves for nine stars. The thick line is the mean extinction curve and the thin line through the data points is the best fit straight line plus Lorentzian to the data (see Section 3). Compared to the mean law HD 52559, 198781 and 185780 have too steep a slope, HD 32990, 37367 and 176819 have a normal slope but an excess 2200 Å feature, and HD 23625, 147165 and 183013 have too shallow a slope. An inspection of the extinction curves shows that there are just two major variations present, (a) the slope of the scattering continuum, and (b) the strength of the 2200 Å feature. Consequently in order to study the variations it was decided to attempt to parameterize the extinction curves in terms of these two components. This analysis is described in the following section.

3 Analysis

Savage (1975) was the first to point out that the mean extinction curve for the wavelength range considered here ($3.65<1/\lambda$ in μm<7.14) can be well represented by a straight line for the scattering component and a Lorentzian for the 2200 Å absorption feature:

$$A(\lambda)/E(B-V)=A+B\times x+G[0.28/\{(x-4.60)^{**}2+0.53^{**}2\}] \quad (1)$$

where $x=1/\lambda$ in micrometres. The central wavelength, $1/\lambda=4.60$ and half-half-width, 0.53, have been taken from Seaton (1979), and for the mean galactic law: $A=2.29$, $B=0.848$, and $G=3.61$.

A least squares fit to each of the 92 anomalous stars was made and the constants A, B and G derived together with their errors. The extinction curves for all the stars could be well fitted by a straight line plus a Lorentzian and with 13 data points the three constants involved (A, B and G) were well determined. For a few stars the far-UV rise in the extinction curve is noticeable with the

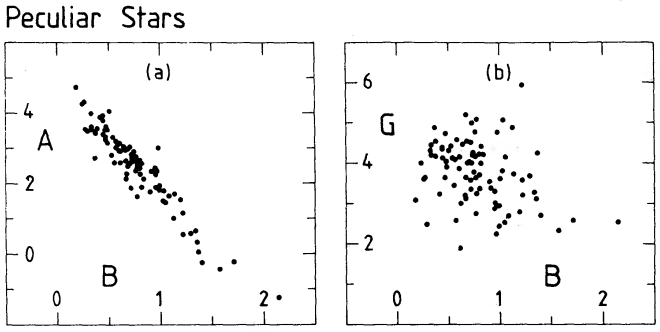


Figure 4. Ninety-two peculiar stars. Extinction curves normalized at B and V. (a) The plot of the intercept, A, against the slope, B. (b) The plot of the 2200 Å feature, G, against the slope, B.

© Royal Astronomical Society • Provided by the NASA Astrophysics Data System

1986MNRAS.219..903C

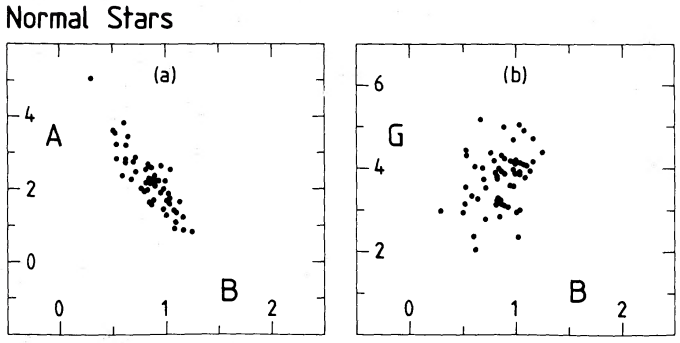


Figure 5. Sixty-two normal stars. Extinction curves normalized at B and V. (a) The plot of the intercept, A, against the slope, B. (b) The plot of the 2200 Å feature, G, against the slope, B.

observed data point lying just above the fit at 1400 Å (7.14 μm^{-1}). If the anomalous extinction curves are all distinct and arise from independent scattering agents then plots of the coefficients (A, B and G) against one another should show no patterns or correlations. If, on the other hand, the extinction curves are members of a family then the plots should show some structure. Fig. 4(a)

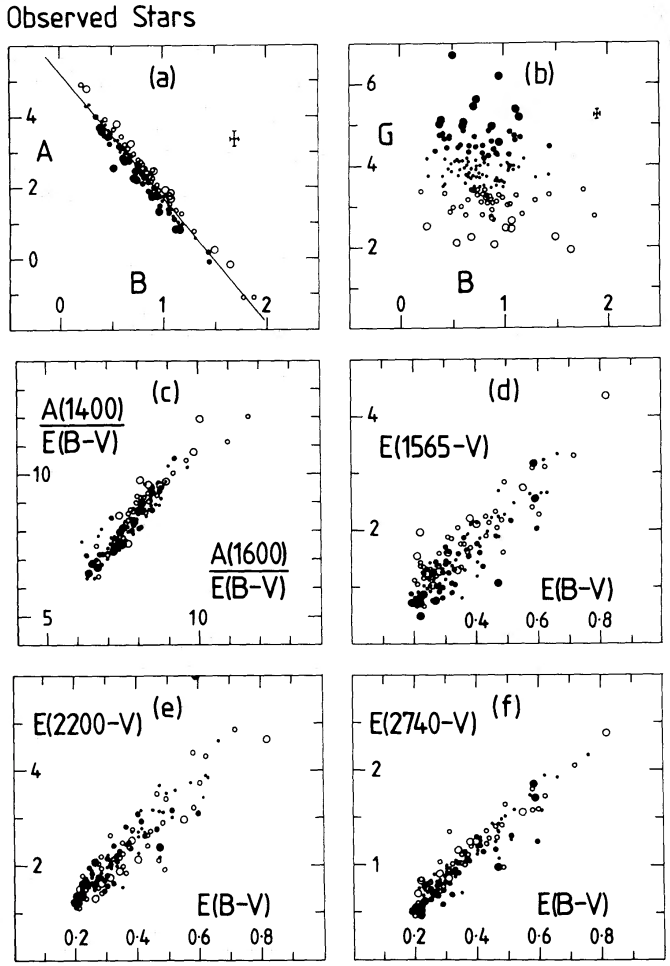


Figure 6. All 154 stars. Extinction curve normalized at V and 2740 Å. The stars are plotted by their 2200 Å strength, varying from strong (filled circles) through normal (dots) to weak (open circles). (a) The plot of the intercept, A, against the slope, B. The line is the best fit to the data. (b) The plot of the 2200 Å feature, G, against the slope, B. (c) The plot of the normalized extinction at 1400 Å against that at 1600 Å. (d) The plot of the colour excess $E(1565-V)$ against $E(B-V)$. (e) The plot of the colour excess $E(2200-V)$ against $E(B-V)$. (f) The plot of the colour excess $E(2740-V)$ against $E(B-V)$.

© Royal Astronomical Society • Provided by the NASA Astrophysics Data System

1986MNRAS.219..903C

shows the plot of the intercept, A, against the slope, B, and the strong linear correlation is clear. A simple physical explanation for this correlation is available. If the scattering extinction is caused by two distinct agents, one having a very shallow slope ($B=0.0$) and the other a very steep slope ($B=2.0$), then these two cases will be represented by a point each in the intercept versus slope diagram. Any actual extinction curve will be a linear combination of these two agents and so give rise to a point lying on the straight line between the two.

Fig. 4(b) plots the strength of the 2200 Å feature, G, against the slope of the extinction curve, B. The plot is a scatter diagram and shows that there is no correlation between the 2200 Å absorption feature and the slope of the scattering continuum. This implies that the agents responsible for the 2200 Å feature and the scattering continuum must be distinct. The smooth variation in Fig. 4(a) and (b) begs the question – how do the normal stars behave? Fig. 5(a) and (b) show the plots for the remaining 62 'normal' stars and it is clear that they mimic the peculiar stars' behaviour.

By normalizing at B and V there is a leverage effect as one goes into the ultraviolet whereby small deviations get magnified. So it is clearly desirable to abandon B as the second normalization point and to choose one in the ultraviolet. The linear variation shown in Figs 4(a) and 5(a) implies that all the scattering curves have the same extinction value near 3200 Å. Hence we choose the broadband photometric channel centred on 2740 Å as the second normalization point, being closest to 3200 Å.

The extinction coefficients A, B, G were recomputed for all 154 stars, again adopting their quoted MK type, but normalizing to 3.20 at V and 6.24 at 2740 Å. Fig. 6(a) plots the intercept, A, against the slope, B, for all 154 stars. Again the strong linear correlation appears. Fig. 6(b) shows the strength of the 2200 Å feature, G, plotted against the scattering slope B, and again there is no correlation.

Two questions have to be answered at this point. First, are the variations within the errors, in which case they are not significant. Secondly, if there is a variation in the shape of the extinction curve, then there should be a correlation between the extinction values at different wavelengths.

First Table 1 gives the values and errors for the extinction coefficients A, B and G for all 154 stars (normalized at V and 2740 Å). The mean values together with their internal (σ) and external (s) errors are:

$A=2.36$	$\sigma=0.20$	$s=0.98$
$B=0.803$	$\sigma=0.032$	$s=0.274$
$G=3.79$	$\sigma=0.13$	$s=0.76$.

The large ratio of s/σ (>5) indicates that the apparent variations are significant. The best fit line to Fig. 6(a) has a gradient of -3.53 so that the family of lines representing possible scattering components to the extinction curve has the form:

$$A(\lambda)/E(B-V)=A+B\times x \qquad (2)$$

where

$$(A-2.36)=-3.53\ (B-3.79).$$

These curves all pass through $A(\lambda)/E(B-V)=5.19$, $x=3.53$, $\lambda=2833$ Å. It should be noted that normalizing the extinction curves to 6.24 at 2740 Å does not force the scattering curves through that point as the 2200 Å feature still makes a significant contribution there. In Fig. 6(a) (where the different symbols denote different 2200 Å strengths) it is clear that stars of all 2200 Å strengths can appear at all slopes, there is no segregation into weak 2200 Å stars at one end and strong 2200 Å stars at the other.

Secondly Fig. 6(c) shows the extinction at 1400 Å plotted against that at 1600 Å. There is a clear

© Royal Astronomical Society • Provided by the NASA Astrophysics Data System

1986MNRAS.219..903C

correlation and hence an *a priori* reason for there being a real variation in the shape of the extinction curve. Again it is to be noted that there is no segregation of stars by their 2200 Å strength.

Having established that the observed variations are significant a third question arises as to whether the variations can be explained by systematic effects, such as spectral type or luminosity class mismatch. This question is dealt with in the next section.

If the interstellar extinction curve has a fixed shape then plots of one colour excess against another will be a straight line through the origin. Fig. 6(d), (e) and (f) plot the observed ultraviolet colour excesses $E(1565-V)$, $E(2200-V)$ and $E(2740-V)$ against the visual colour excess $E(B-V)$. All of them show a rough linear relationship and the slope of the best fit line through the origin defines the mean extinction curve through the relation:

$$A(\lambda)/E(B-V)=E(\lambda-V)/E(B-V)+R \tag{3}$$

where $R=A(V)/E(B-V)=3.20$. In the past the observed linear relationships of Fig. 6(d), (e) and (f) have been used to justify the concept of a mean extinction law, and the scatter of points about each line has been explained in terms of the observational errors and systematic effects. The next section shows that Fig. 6 cannot be explained by observational errors and systematic effects, that a varying extinction law is required, and that the form of the variation will give rise to the apparent linear relationships seen in Fig. 6(d), (e) and (f).

4 Systematic errors

Systematic effects can arise from a number of sources. Observational errors in the magnitudes at the normalization points (V, B, or 2740 Å) result in an erroneous scale for the extinction with the extinction curve becoming either stretched or compressed in the $A(\lambda)/E(B-V)$ direction. Errors in spectral class also lead to erroneous $E(B-V)$ values with similar scaling effects. Both of these give leverage effects whereby a small error close to the normalization points becomes amplified into much larger errors further away. Errors in luminosity class can lead to drastic changes in the slope of the extinction curve, especially if the star is a supergiant (hence the deliberate exclusion of luminosity classes Ia to II–III). It is difficult to take account of the effects of systematic errors in the analysis in a direct manner. However, with a grid of intrinsic colours and a simple algebraic expression for the extinction law, it is a straightforward matter to generate random samples of 'synthetic stars' which can be compared with the observations. Three random samples of stars were generated having the following properties:

(i) *Spectral Class Errors.* A sample of luminosity class III, IV and V stars with a spectral classification error of one subclass, e.g. B1V misclassified as B0V or B2V, B2III misclassified as B1III or B3III, etc.

(ii) *Luminosity Class Errors.* A sample of luminosity class III and V stars with spectral classification errors as for sample 1. In addition all class III stars were misclassified as class V, and all class V stars misclassified as class III.

(iii) *Supergiant Errors.* A sample of class Ia supergiant stars with spectral classification errors as for sample 1. In addition all the stars were misclassified as either luminosity class III or V.

The samples were constructed as follows. A random MK type was selected and its intrinsic colours reddened using the mean extinction law to an $E(B-V)$ chosen randomly in the range 0.2–0.8. Random errors with a standard deviation of 0.03 were added to the B and V magnitudes, and a random error with a standard deviation of 0.10 added to the 2740 Å magnitude. This gave a reddened spectrum with random photometric error on V, B and 2740 Å. A second random MK type was then selected for the comparison star giving the required classification error and

© Royal Astronomical Society • Provided by the NASA Astrophysics Data System

1986MNRAS.219..903C

allowing the extinction curve to be constructed by the 'pair method'. The extinction curve, after normalizing to 3.20 at V and 6.24 at 2740 Å, was fitted with a linear scattering component and a Lorentzian 2200 Å feature to give the A, B and G parameters. The properties of the three samples are now discussed in turn.

4.1 SPECTRAL CLASS ERRORS

Fig. 7(a) shows the plot of slope, B, against intercept, A, for sample 1. The diagram is similar in shape to the observed stars, Fig. 6(a), but there is now a clear segregation of stars with strong 2200 Å stars, filled circles, having a steep slope and weak 2200 Å stars, open circles, having a shallow slope. For clarity all the diagrams illustrating the systematic effects only show the normal, very strong, and very weak 2200 Å points, the intermediate strong and weak points being omitted. Fig. 7(b) shows the plot of 2200 Å-strength against the scattering slope. The strong correlation seen is responsible for the segregation by 2200 Å strength observed in Fig. 7(a), and the diagram is clearly inconsistent with the observations. Fig. 7(c) shows the extinction at 1400 Å plotted against that at 1600 Å. There is a good correlation similar to that seen in Fig. 6(c), but there is also a clear segregation of stars by their 2200 Å strength, not seen in the observed stars,

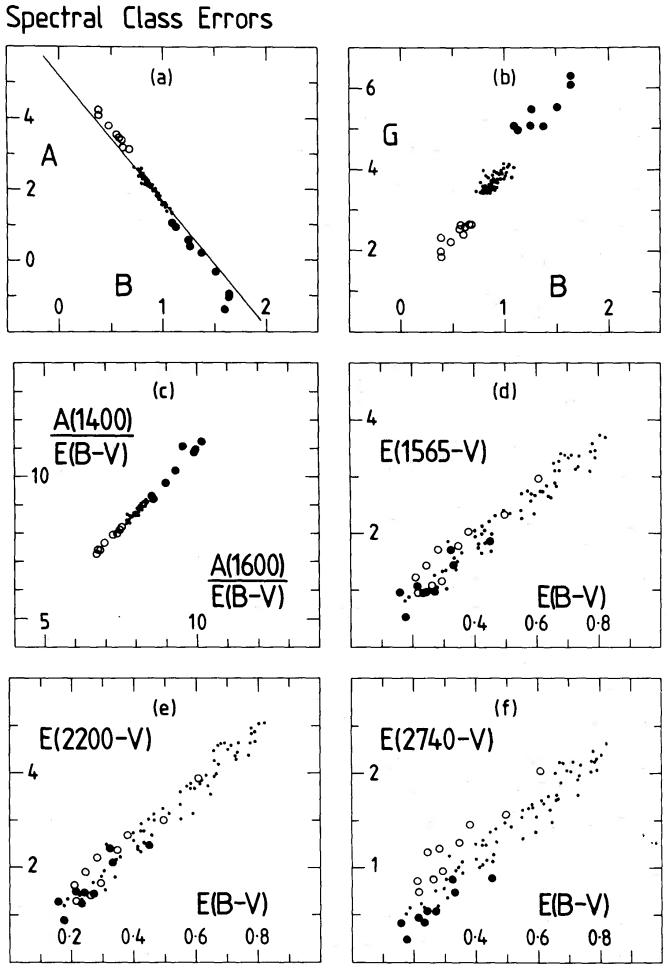


Figure 7. Plots corresponding to Fig. 6 for a random sample of stars having spectral classification errors. For clarity only the strong 2200 Å points (filled circles), normal (dots), and weak (open circles) are shown. The line in 7(a) is the best fit to the observed stars shown in 6(a).

© Royal Astronomical Society • Provided by the NASA Astrophysics Data System

1986MNRAS.219..903C

Fig. 6(c). Fig. 7(d), (e) and (f) are very similar to 6(d), (e) and (f) with approximately the same degree of scatter.

This sample of stars demonstrates that the observations cannot be explained by a fixed extinction curve, photometric errors in V, B and 2740 Å, and errors in spectral class.

4.2 LUMINOSITY CLASS ERRORS

Fig. 8(a) shows the plot of slope against intercept for sample 2. The diagram shows the same distribution as for the observed stars, Fig. 6(a), but the clear segregation of stars by their 2200 Å strength as found in Fig. 7(a) is present. Fig. 8(b) shows the correlation between 2200 Å strength and scattering slope. This is similar to Fig. 7(b) with an enhanced scatter, but it is still completely at variance with the observations as shown in Fig. 6(b). Fig. 8(c) is similar to 7(c), with the segregation of stars by their 2200 Å strength, again at variance with the observations, Fig. 6(c). Fig. 8(d), (e) and (f) are very similar to the spectral class error stars of Fig. 7(d), (e) and (f), with roughly the same degree of scatter. There is, however, an added tendency for the strong 2200 Å points to be low and the weak 2200 Å points to be high, a separation not seen in the observations, Fig. 6(d), (e) and (f). And there is a tendency for the strong 2200 Å points to occur only at small $E(B-V)$ values.

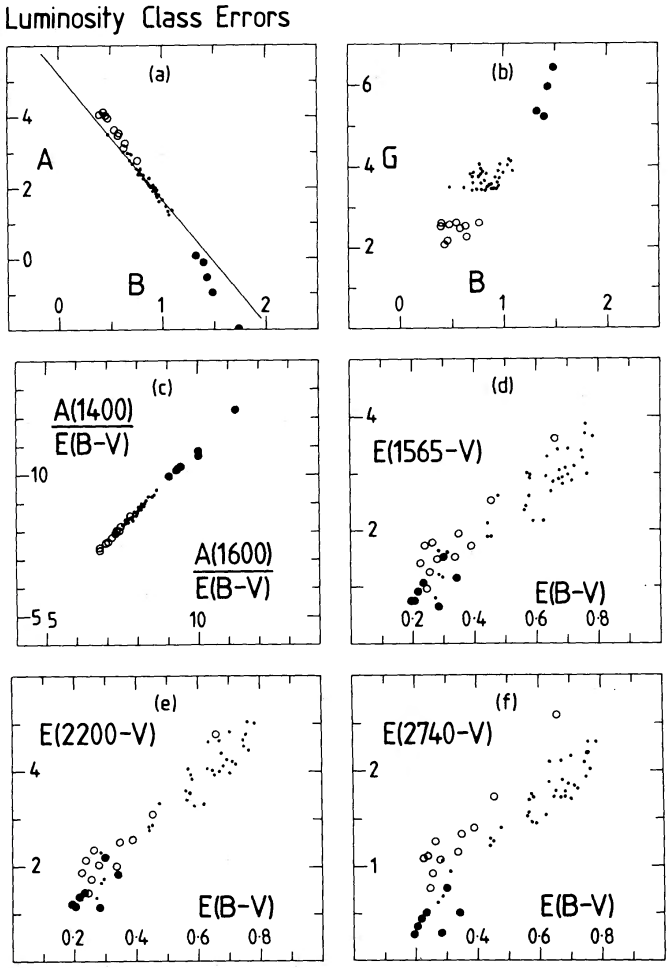


Figure 8. Plots corresponding to Fig. 6 for a random sample of stars having luminosity classification errors. The line in 8(a) is the best fit to the observed stars shown in 6(a).

© Royal Astronomical Society • Provided by the NASA Astrophysics Data System

1986MNRAS.219..903C

This sample of stars demonstrates that the observations cannot be explained through simple luminosity class errors whereby class III stars are misclassified as class V and vice-versa. This is as expected in that there are relatively small differences between the intrinsic colours of class III, IV & V stars in the ultraviolet.

4.3 SUPERGIANT ERRORS

The observed set of 154 stars have MK luminosity classes III to V. Hence in considering the effect of supergiants it is only necessary to consider class Ia (strictly Ia through II–III) stars misclassified as class III, IV or V, as any misclassifications the other way round would not appear in the observed set. Fig. 9(a) gives the slope versus intercept diagram. It shows that misclassified supergiants give rise to systematically large scattering slopes with no points occurring with slope shallower than the observed mean value. There is also the segregation of stars by their 2200 Å strength with, again, the steeper slopes having the stronger 2200 Å feature. Fig. 9(b) shows the 2200 Å strength versus scattering slope and it is similar to that of 7(b) and 8(b) except that the stars have been shifted to steeper slopes, and there is a larger scatter. Compared to the observations, Fig. 6(b), these points occur too far to the right in regions where (for strong 2200 Å points) there

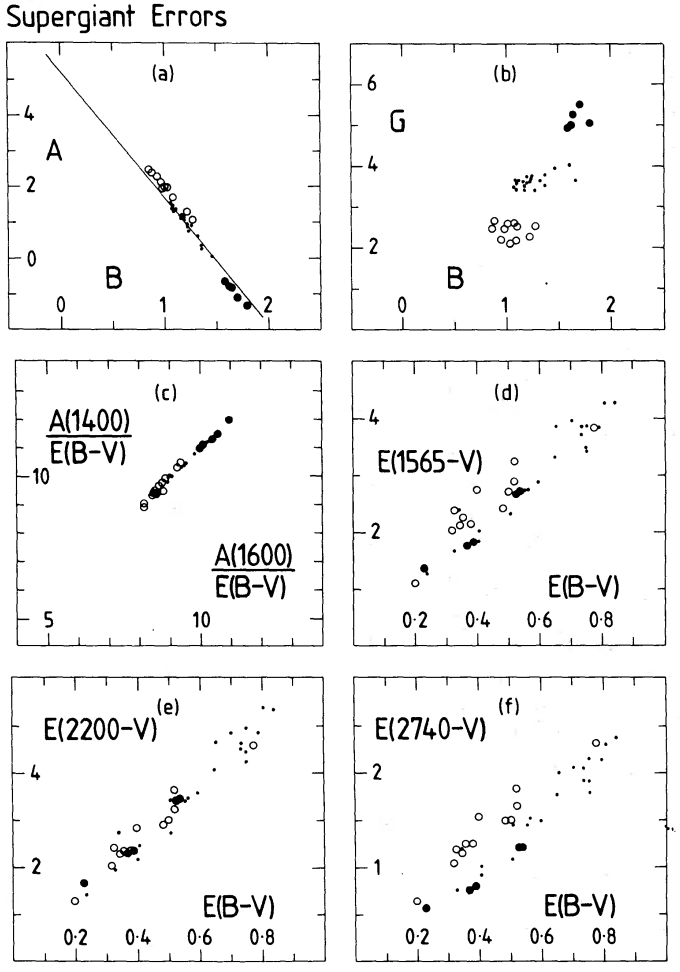


Figure 9. Plots corresponding to Fig. 6 for a random sample of supergiants misclassified as class III or V stars. The line in 9(a) is the best fit to the observed stars shown in 6(a). The lines in 9(d), (e) and (f) show the mean extinction law of Seaton (1979).

© Royal Astronomical Society • Provided by the NASA Astrophysics Data System

1986MNRAS.219..903C

are no observed stars at all. Fig. 9(c) shows the plot of extinction at 1400 Å versus that at 1600 Å. The segregation by 2200 Å strength is still present though not as marked as for the spectral class error and luminosity class error samples. The extinction values tend to be larger than the observations with if anything a negative correlation in the sense that the strong 2200 Å points occur in the region where observationally only weak stars are seen. Fig. 9(d), (e) and (f) are similar in form to 8(d), (e) and (f). However, the low-lying nature of the strong 2200 Å points and high position of the weak 2200 Å points is more marked and completely at variance with the observations.

So once again the detailed behaviour of the observed stars cannot be explained in terms of supergiant stars being misclassified as giant or main sequence stars. These three samples of random stars demonstrate that normal photometric errors on V, B and 2200 Å, and normal spectral type or luminosity class errors cannot explain the observed variations seen in the interstellar extinction curves. And the conclusion reached earlier that the extinction curve must be made up of at least two components that vary independently of one another still stands.

Figs 7(b), 8(b) and 9(b) all show a strong positive correlation between the scattering slope and the strength of the 2200 Å feature. They show that for photometric errors, spectral type and luminosity class errors, stars with steep scattering slopes have a strong 2200 Å feature, and vice-versa, stars with shallow scattering slopes have a weak 2200 Å feature. It follows that, whatever the true distribution of scattering slope against 2200 Å strength, the observed distribution will be stretched from bottom left to top right. So an interpretation of Fig. 6(b) is that the true distribution of slope against 2200 Å strength is from top left to bottom right, and the observational errors stretch this line across its width to give the observed scatter diagram.

5 The profile of the 2200 Å feature

The usual method for deriving the profile of the 2200 Å feature is to start with the extinction curve and to assume a form for the underlying scattering continuum, such as a linear law between 1500 and 2800 Å. The profile is then simply given by subtracting this continuum from the extinction curve. This clearly means that the profile depends on the shape of the adopted underlying continuum. However, if the extinction curve varies, then the profile can be derived without any assumptions about the underlying scattering continuum. A star with a normal scattering extinction but an excess 2200 Å feature will have an extinction curve that differs from the mean curve by the 2200 Å profile. Within the sample of 154 there are 13 stars that have a scattering slope within one standard deviation of the mean slope with a 2200 Å excess greater than one standard deviation. These 13 stars (HD 2654, 8965, 21856, 27192, 54439, 144470, 149363, 163472, 181963, 192539, 201795, 204150, and 218376) can be used to determine the 2200 Å profile. The best fit spectral type for each star was redetermined (as described in Section 1 but restricted to within one subclass of the cited spectral class) using the visible points (U, B, V), and the ultraviolet points shortwards of 1750 Å, i.e. the data points across the 2200 Å feature were omitted. The extinction curve was then given by differencing the observed colours, $[m(\lambda)-V]$, from the intrinsic colours for the best fit, and normalizing to 3.20 at V and 4.20 at B. The 2200 Å profile then followed as the simple difference between the star's individual extinction curve and the mean curve. The resultant profile, derived from all 13 stars, is tabulated in Table 2 and shown in Fig. 10, where the solid line is the best fit line plus Lorentzian:

$$r(\lambda)=-0.051-0.005x+0.262/[(x-4.568)^{**}2+0.229] \quad (4)$$

where $r(\lambda)$ is the profile normalized to 1.0 at 2200 Å, and x is in μm^{-1}.

It is to be noted from Table 2 that the external (scatter) error is smaller than the internal (photometric) error at nearly all wavelengths. This indicates that the profile is well determined

© Royal Astronomical Society • Provided by the NASA Astrophysics Data System

1986MNRAS.219..903C

Table 2. 2200 Å profile. The profile of the 2200 Å feature. $r(\lambda)$ is the value of the straight line plus Lorentzian fit normalized to 1.00 at 2200 Å. Sig is the internal error and scat the external scatter error.

WavL	1/λ	r(λ)	sig	scat
1400	7.14	-0.048	0.048	0.024
1500	6.67	-0.009	0.046	0.016
1600	6.25	0.043	0.047	0.019
1700	5.88	0.086	0.044	0.017
1800	5.56	0.212	0.039	0.036
1900	5.26	0.282	0.040	0.054
2000	5.00	0.567	0.041	0.037
2100	4.76	0.928	0.042	0.053
2200	4.55	1.000	0.045	0.039
2300	4.35	0.914	0.042	0.032
2400	4.17	0.603	0.039	0.018
2500	4.00	0.398	0.036	0.041
2740	3.65	0.152	0.019	0.026
3650	2.74	-0.005	0.031	0.020
4400	2.27	0.050	0.031	0.013
5500	1.82	-0.048	0.031	0.018

and shows no signs of variation. In fitting each extinction curve to a straight line plus a Lorentzian no attempt was made to allow for variations in the position or width of the Lorentzian. A central wavelength of 4.6 μm^{-1} and half-half-width of 0.53 were assumed for all stars. A visual inspection of the 154 extinction curves did not reveal any 2200 Å features that showed obvious or significant departures. However, a proper determination of the central wavelength and half-width for each curve (together with their errors) would allow a full statistical examination to be made of any variations and this perhaps should be carried out in the near future. In conclusion the 2200 Å

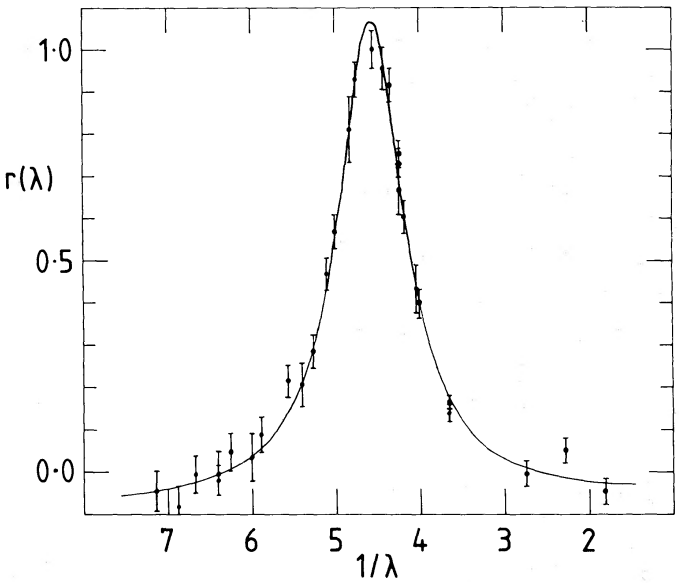


Figure 10. The profile of the 2200 Å feature as derived from 13 stars showing a 2200 Å excess. The thin line is the best fit straight line plus Lorentzian.

© Royal Astronomical Society • Provided by the NASA Astrophysics Data System

1986MNRAS.219..903C

Table 3. Other anomalous stars. Forty-four stars reported by other authors as having anomalous extinction curves. HD numbers marked with an asterisk are common to Table 1. A, B, sA, sB are the intercept, slope and errors for the linear scattering part of the star's individual extinction curve. Very steep or very shallow lines are marked by ++ or −− respectively, and steep or shallow lines by + or −. G and sG are the magnitude and error of the Lorentzian fit to the 2200 Å feature. Very strong or very weak 2200 Å are marked by ++ or −−, and strong or weak 2200 Å by + or −. The number in the Refs column identifies the source. (1) Bless & Savage 1972; (2) Morales *et al.* 1980; (3) Snow & Seab 1980; (4) Meyer & Savage 1981; (5) Bohlin & Savage 1981; (6) Seab *et al.* 1981; (7) Massa *et al.* 1983; (8) Witt *et al.* 1984; (9) Seaton 1979; (10) Nandy *et al.* 1981; (11) Bromage & Nandy 1983.

HD	MK Type	V	E(B-V)	A	sA	B	sB		G	sG		Refs
1337	O 9 II-III	6.05	0.23	0.0	.2	1.55	.04	++	3.0	.1	-	4, A0 Cas
21291	B 9 Ia	4.21	0.41	1.6	.3	0.93	.04		4.9	.2	++	8
21803*	B 2 IV	6.41	0.27	0.9	.2	1.15	.03	+	4.7	.1	+	2
24398	B 1 Ib	2.85	0.31	3.2	.2	0.59	.03	-	3.8	.1		1, ζ Per
24432	B 3 II-III	6.82	0.75	1.5	.3	1.17	.05	+	1.9	.3	--	4,7
27192*	B 2 IV	5.55	0.23	2.2	.2	0.74	.03		5.6	.1	++	2
29647	B 8 III	8.11	1.06	2.7	.3	0.95	.06	+	0.3	.3	--	3,6
32990*	B 2 V	5.50	0.30	2.6	.1	0.73	.02		3.9	.1		2
34078	O 9.5 V	5.95	0.52	3.9	.2	0.41	.03	-	3.2	.1	-	8
37367*	B 2 V	5.95	0.40	2.7	.1	0.66	.02	-	4.5	.1	+	2,4,7
37903*	B 1.5 V	7.82	0.35	3.6	.2	0.42	.04	-	3.5	.1		7,8
38087	B 5 V	8.30	0.29	5.1	.3	-0.13	.04	--	5.6	.2	++	8
38131	B 0.5 V	8.19	0.49	2.5	.3	0.83	.04		2.5	.2	--	8
40893	B 0 IV	8.90	0.46	2.1	.3	0.89	.05		3.7	.2		8
42379	B 1 II	7.39	0.59	1.6	.2	1.11	.03	+	2.6	.1	--	4
45910	B 4 I-II	6.78	0.57	3.4	.1	0.68	.03		2.1	.1	--	4
53367	B 0 IV	6.96	0.74	3.7	.2	0.50	.04	-	2.9	.2	-	8
53974*	B 0.5 III	5.38	0.32	1.5	.2	1.04	.03	+	3.9	.1		8
73882	O 8 V	7.20	0.70	2.6	.2	0.85	.03		2.3	.1	--	4,7
110432	B 1.5	5.32	0.51	2.2	.2	0.87	.03		3.3	.1	-	4
143275	B 0 IV-V	2.31	0.19	4.4	.2	0.29	.04	--	3.1	.1	-	1, δ Sco
144217	B 0.5 V	2.53	0.20	3.6	.2	0.45	.03	-	3.7	.1		1, β Sco
147165*	B 1 III	2.87	0.40	4.3	.2	0.27	.03	--	3.7	.1		1,4, σ Sco
147889	B 2.5 V	7.89	1.08	5.6	.4	0.10	.06	--	0.8	.3	--	4,5,6
147933	B 2 IV	4.61	0.47	3.7	.2	0.38	.03	--	5.0	.1	++	1,4,6, ρ Oph
148184	B 2 IV-V	4.38	0.53	3.9	.1	0.42	.02	-	3.2	.1	-	4
149757	O 9 V	2.57	0.33	2.9	.2	0.72	.03		2.8	.1	-	1, ζ Oph
167264	B 0 Ia	5.37	0.30	3.9	.2	0.33	.03	--	4.4	.1	+	4
167835	B 5 Ia	6.73	0.55	1.8	.2	0.85	.04		5.3	.2	++	8
169454	B 1 Ia	6.61	1.13	1.9	.2	1.05	.03	+	2.0	.1	--	6
169753	B 2.5 III	7.53	0.84	2.5	.3	0.94	.07	+	1.1	.3	--	4
170740*	B 2 V	5.72	0.48	2.5	.1	0.79	.02		3.3	.1	-	8
183143	B 7 Ia	6.87	1.26	5.2	.4	0.27	.07	--	0.4	.3	--	6
183561	B 2 III	8.05	0.41	2.4	.3	0.84	.05		3.1	.2	-	4
185859	B 0.5 Iab	6.50	0.61	3.2	.1	0.51	.02	-	4.7	.1	+	4
190603	B 1 Ia	5.63	0.72	1.6	.1	1.02	.02	+	3.5	.1		8
192001	O 9.5 IV	8.25	0.62	1.9	.3	1.02	.05	+	2.1	.2	--	4
197460	B 0.5 I-II	8.14	0.56	2.4	.3	0.94	.05	+	1.8	.2	--	4
197512	B 1 V	8.56	0.32	3.4	.2	0.59	.03	-	3.1	.1	-	8
200775	B 2 V	7.33	0.62	4.0	.1	0.49	.02	-	1.6	.1	--	4
207198	O 9 I-II	5.94	0.58	2.2	.2	0.94	.03	+	2.7	.1	-	4,7
210072	B 2 V	7.66	0.54	0.7	.2	1.40	.04	++	1.5	.2	--	4,7
225146	B 0 Ib	8.59	0.60	3.6	.4	0.66	.07	-	1.0	.3	--	8
235795	B 1.5 V	9.14	0.18	-0.5	.8	1.50	.12	++	5.7	.6	++	4
GALAXY				2.3		0.85			3.6			9
LMC				1.0	.8	1.37	.15		1.7	.5		10
SMC				1.5	1.8	1.33	.29		0.2	1.0		11

© Royal Astronomical Society • Provided by the NASA Astrophysics Data System

1986MNRAS.219..903C

profile is symmetrical and consistent with a Lorentzian centred on 2190 Å and full-half-width of 460 Å.

6 Other anomalous stars

About 100 stars have been reported by various authors as having anomalous extinction curves in the ultraviolet (Bless & Savage 1972; Willis & Wilson 1975, 1977; Savage *et al.* 1978; Morales *et al.* 1980; Seab, Snow & Joseph 1980; Bohlin & Savage 1981; Meyer & Savage 1981; Seab *et al.* 1981; Massa *et al.* 1983; Witt *et al.* 1984). Sixty-nine of these were found to have been observed by the S2/68 ultraviolet sky telescope. After eliminating those with poor quality data and those with no available intrinsic colours (Wolf–Rayet and Be stars), a total of 44 stars remained for which extinction curves could be constructed. The extinction curves were computed as before, by differencing the observed $m(\lambda)-V$ colours with the intrinsic colours for the same MK spectral type, and normalizing to 3.20 at V and 6.24 at 2740 Å. The best fit straight line plus Lorentzian to the extinction curve was derived using least squares to give the intercept, A, slope, B, and 2200 Å strength, G. The value and errors for all 44 stars are given in Table 3. Of these 44 stars, eight are common to the original selection of 154 stars (marked by an asterisk in Table 3), six are O-type stars, 14 have luminosity classes in the range Ia to II–III, two are reddened less than $E(B-V)=0.20$, and the remaining 14 have an MK spectral type that is inconsistent with the cited UBV photometry. Also listed in Table 3 are the extinction parameters for the Galaxy and the Magellanic Clouds. The extinction curves for all the anomalous stars could be well fitted by a straight line plus Lorentzian. The worst case occurs for HD 37903 where the curvature of the far-UV rise begins to depart from the straight line approximation. However, no extinction curves were found that were so radically different that they could not be fitted by a straight line plus Lorentzian.

Fig. 11(a) shows the plot of the intercept, A, against the slope, B, for all 44 anomalous stars. The same linear correlation is found as for the observed stars, Fig. 6(a), and again there is no segregation along the line by 2200 Å strength. There is, however, an apparent splitting across the line whereby weak 2200 Å stars all lie above the line and all strong 2200 Å stars lie below. This trend also occurs for the observed stars but is less clear. This separation is explained as a consequence of the normalization at 2740 Å. The 2200 Å feature can make a small but significant contribution to the flux at 2740 Å and this contribution will affect points in Fig. 12(a) in the sense observed. It is interesting to note the position of the Magellanic Clouds which, within the errors, lie on the line of the galactic stars. And the SMC with its weaker 2200 Å feature lies further away from the line than the LMC, as expected from the effect of normalizing at 2740 Å.

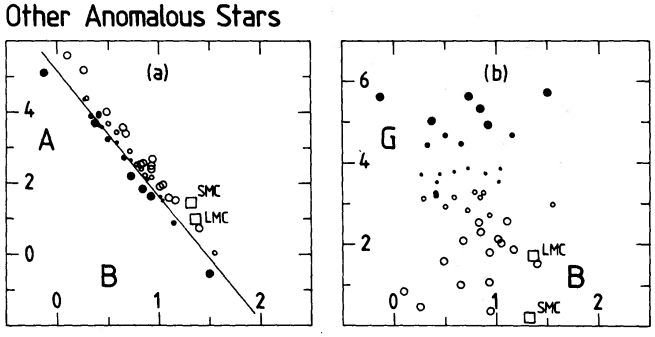


Figure 11. Plots corresponding to Fig. 6 for 44 stars cited by other authors as having anomalous extinction curves. (a) The plot of intercept, A, against slope, B. The line is the best fit to the observed stars shown in 6(a). (b) The plot of 2200 Å feature, G, against slope, B.

© Royal Astronomical Society • Provided by the NASA Astrophysics Data System

1986MNRAS.219..903C

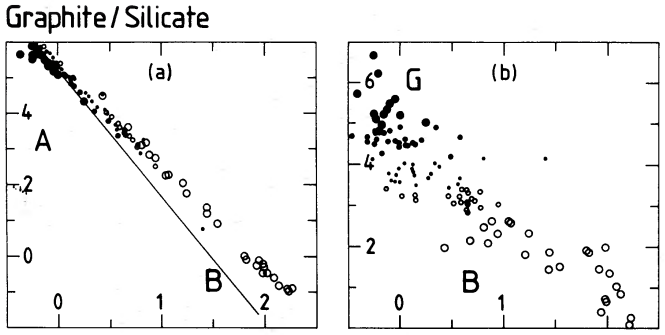


Figure 12. Random sample of stars and a varying extinction curve made from differing proportions of graphite and silicate grains. (a) The plot of intercept, A, against slope, B. The line is the best fit to the observed stars shown in 6(a). (b) The plot of the 2200 Å feature, G, against the slope, B. In both diagrams pure graphite lies to the top left and pure silicate to the bottom right.

Fig. 12(b) shows the variation of 2200 Å strength, G, with scattering slope, B. The plot is similar to that of the observed stars, Fig. 6(b). However, the very strong and very weak 2200 Å stars have a wider scatter and there are many more weak stars. This is not altogether surprising as these 44 stars have been selected for their anomalous extinction, whereas the starting sample of 154 stars has no such bias.

7 Grain models

Several attempts have been made to reproduce the observed mean extinction curve theoretically (e.g. Mathis, Rumpl & Nordsiek 1977; Draine & Lee 1984). These models usually assume two types of grains, and recently Draine & Lee have arrived at a combination of graphite and an artificial 'astronomical' silicate. With two grain types one can go further than merely fitting the fixed mean extinction curve, by attempting to model the apparent variations. We assume that the observed variations arise from three sources, (a) observational error, (b) different chemistry or grain type, and (c) different size distributions. To investigate the effects of different grain size distributions one requires, of course, detailed model calculations which are beyond the scope of this paper. However, by adopting the extinction curves for graphite and silicate of Draine & Lee and, by varying the relative proportion of each, we can to a limited extent examine the effects of observational error and variable chemistry. A sample of random stars was generated exactly as for the classification error sample described in Section 4, i.e. luminosity class III to V with normal photometric and classification errors. The extinction curve was generated by randomly selecting the proportions of graphite and silicate. The resultant plot of intercept, A, against scattering slope, B, is shown in Fig. 12. The linear correlation is well reproduced although the points do not lie along the same line as galactic stars. There is also a separation of stars by their 2200 Å strength. This separation is to be expected since, for no observational errors, there would be a perfect separation with the pure graphite (strong 2200 Å) points lying close to $B=0$, and the pure silicate (zero 2200 Å) points lying beyond $B=2$. The observational errors tend to smear out this separation, but not to the extent actually observed.

Fig. 12 shows the variation of 2200 Å strength, G, with scattering slope, B. With no observational errors the points would lie along the straight line illustrated, between strong 2200 Å and shallow slope and weak 2200 Å and strong slope. It is seen that the errors are capable of introducing a scatter that is comparable with the observations, Fig. 6(b). However, there is still a clear linear correlation in Fig. 12(b) that is not seen in Fig. 6(b). As noted before the diagrams for the three samples of random error stars [Figs 7(b), 8(b) and 9(b)] all show a linear correlation

© Royal Astronomical Society • Provided by the NASA Astrophysics Data System

1986MNRAS.219..903C

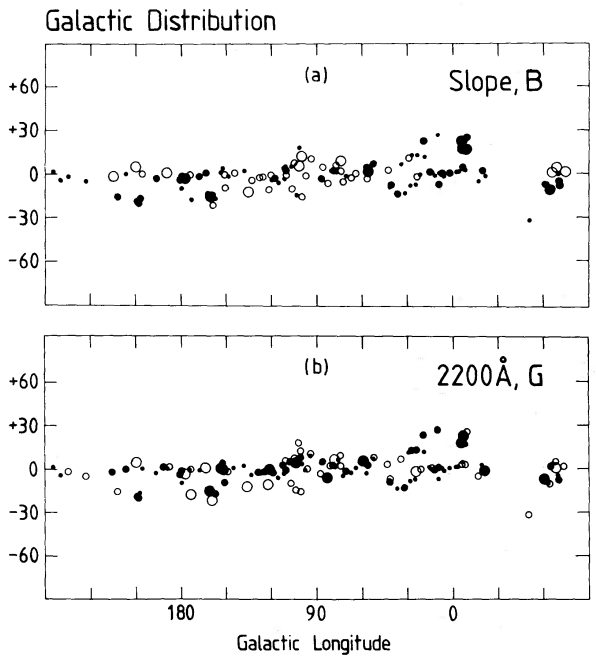


Figure 13. (a) The galactic distribution of the scattering slope, B. Filled circles indicate shallow slopes, dots normal slopes, and open circles strong slopes. (b) The galactic distribution of the 2200 Å strength, G. Filled circles indicate strong 2200 Å, dots normal, and open circles weak.

between 2200 Å strength and scattering slope in the opposite sense to the grain models of Fig. 13(b). For these diagrams the points lay between bottom left and top right, whereas now all the points lie between top left and bottom right.

In conclusion it is clear that the two-grain model goes some way towards explaining the observations. It would be interesting to see what would happen to Fig. 13(a) and (b) if variations in the grain size distributions were also introduced.

8 Galactic distribution

If the variations in the extinction curve are caused by variations in the types of grain along the line-of-sight then we would expect to find that stars close together on the sky exhibit similar extinction characteristics. Fig. 13(a) shows the galactic distribution of the scattering slope, B, where the open circles indicate steep slopes and the filled circles shallow slopes. There are no large regions with similar scattering slopes, though on the small scale one can find several areas where the stars do show either weak or strong slopes. Fig. 13(b) shows the galactic distribution of the 2200 Å strength, G, where the open circles indicate a weak 2200 Å feature and the filled circles a strong 2200 Å feature. Again there are no obvious regions where all the stars are either strong or weak. A comparison by eye of Fig. 13(a) and (b) reveals many small regions where both figures have similar symbols, either filled or open circles. This indicates that there is a slight tendency for stars with steep scattering slopes to have a weak 2200 Å feature, and vice-vera, for stars with shallow slopes to have a strong 2200 Å feature.

It is important at this point to ask whether we should really expect there to be any correlations between the scattering slope and 2200 Å strength with galactic position or any other interstellar parameter including $E(B-V)$ or the strength of the 4430 Å diffuse interstellar feature. If the extinction is caused by different agents then we should expect correlations between the shape of the extinction curve and the amount of each agent present. However, in expressing the extinction

© Royal Astronomical Society • Provided by the NASA Astrophysics Data System

1986MNRAS.219..903C

curve as a straight line plus a Lorentzian we are treating it mathematically and not physically. Ideally, if the extinction curve is caused by two different agents, then we should express the curve in terms of their individual extinction curves. For example, if the 2200 Å feature is caused by graphite, then the 2200 Å feature should not be treated on its own as a pure Lorentzian but should instead have an additional linear component to account for the graphite extinction at other wavelengths. But even so, if the 2200 Å feature is caused by one agent, then we should expect a weak correlation between the strength, G, and galactic position rather than no correlation at all, and this is perhaps what we observe.

An attempt was made to see whether the 2200 Å strength or the scattering slope was correlated with the 4430 Å feature. Ninety-one of the 154 stars studied have 4430 Å measurements in the catalogue of Snow, York & Welty (1977). The resultant plot between the depth of the 4430 Å feature and the strength of 2200 Å was a scatter diagram. The correlation coefficient was found to be 0.25 indicating that there is no correlation at all. A similar scatter diagram was obtained by plotting the depth of 4430 Å against the extinction at 1500 Å (which essentially measures the slope of the extinction curve). The correlation coefficient was −0.18, again indicating no correlation. However, as mentioned above, one is essentially comparing a physical parameter, 4430 Å depth, against an algebraic parameter, A or G, and the lack of correlation is perhaps not too surprising.

9 Correcting for extinction

A knowledge of the mean interstellar reddening curve is important in correcting observations for extinction effects. If the extinction varies then it is important to know how often curves differ significantly from the mean. In this respect several authors have remarked that caution must be used when correcting individual stars if large errors in the dereddened fluxes are to be avoided (e.g. Bohlin & Savage 1981; Meyer & Savage 1981). Meyer & Savage examined 1367 stars observed by the *ANS* satellite and listed 58 stars (4 per cent) with peculiar extinction curves. If we exclude O-type stars, supergiants, emission line and peculiar stars (which can give large errors in the extinction curve) this list is reduced to just 16 stars, or 1 per cent. One per cent (or even 4 per cent) cannot be regarded as common and on this basis the adoption of a mean curve for the correction of extinction effects is justified.

The numerical handling of the extinction curve used in this paper, together with the fact that the sample of 154 stars is homogeneous, complete and contains no bias towards anomalous extinction stars, allows us to study the problem of correcting observations quantitatively. We consider an extinction curve to be peculiar if it differs from the mean curve by more than 1 mag. Such a deviation will give rise to a 1 mag error in the star's dereddened fluxes for an extinction of $E(B-V)=1.0$. For simplicity we restrict the deviation by 1 mag at either 1500 or 2200 Å. On this basis 42 stars are peculiar at 1500 Å and 35 stars at 2200 Å or together approximately one star in three has an extinction curve that deviates significantly from the mean, a much higher proportion than that found by Meyer & Savage or other authors.

With such a high proportion of deviating extinction curves it is desirable to be able to check the extinction curve for any individual star. If the extinction curves are normalized to 3.20 at V and 4.20 at B [i.e. $E(B-V)=0.0$], then the mean values of the extinction parameters, for use in equation (1), are $A=2.36$, $B=0.805$,$G=3.73$. The scattering line for an individual extinction curve is approximately given by:

$$B=0.28\,E(1500-V)/E(B-V)-0.53, \tag{5}$$

$$A=4.86-3.10\,B.$$

If one prefers a value of $R=A(V)/E(B-V)=3.1$ (in place of the 3.2 adopted here) the constant of 4.86 in equation (5) should simply be replaced by 4.76.

© Royal Astronomical Society • Provided by the NASA Astrophysics Data System

1986MNRAS.219..903C

Table 4. Intrinsic ultraviolet colours. The intrinsic $[m(1500)-V]$ and $[m(2200)-V]$ colours for O9 to B5 stars.

	m(1500)-V			m(2200)-V		
MK	Ia	III	V	Ia	III	V
O9	-	-4.46	-4.41	-	-3.54	-3.48
B0	-3.58	-4.35	-4.43	-2.99	-3.40	-3.39
B1	-3.04	-3.94	-3.97	-2.61	-3.07	-2.98
B2	-2.80	-3.57	-3.64	-2.35	-2.78	-2.75
B3	-2.30	-3.21	-3.24	-1.93	-2.38	-2.35
B4	-2.06	-2.85	-3.06	-1.72	-2.10	-2.20
B5	-1.81	-2.59	-2.86	-1.51	-1.85	-2.02

The scattering extinction can be considered normal if $0.53<B<1.09$. Likewise the 2200 Å strength for an individual extinction curve is approximately given by:

$$G=1.01\,E(2200-V)/E(B-V)-2.85. \quad (6)$$

The 2200 Å feature can be considered normal if $2.73<G<4.73$. If B and G are either both low or both high then there is a strong possibility that the MK spectral type or UBV photometry are in error, since these combinations occur naturally as a consequence of photometric or spectral classification errors (see Section 4). To aid the evaluation of A, B and G, a reduced set of intrinsic $[m(1500)-V]$ and $[m(2200)-V]$ colours are given in Table 4; a complete set is given by Carnochan (1982). If the extinction curve appears anomalous then the observations can be corrected using the A, B and G values and equation (1). Alternatively, and better, the actual extinction curve should be derived, fitted with a straight line plus Lorentzian, and the constants A, B and G determined by least squares. It must be noted that equation (1) only holds for the wavelength range 1350–2740 Å.

10 Discussion

The basic conclusion of this paper is that the interstellar extinction curve does vary and that significant deviations from the mean curve are common. That the extinction curve does vary should not be surprising. Indeed since variations in stellar type and in the conditions in the interstellar medium are widespread we should expect some variation in the populations of interstellar grains, and hence in the shape of the extinction curve. A wider examination of the variations within the limits of the S2/68 sky survey would be extremely useful. This can be accomplished by extending the sample to stars more luminous than class III and to stars less reddened than $E(B-V)=0.20$.

If variations in the extinction curve are so common then we have to answer the question of why they were not detected earlier. There are many reasons for this.

(i) To demonstrate a variation it is necessary to compute two errors, internal and external, and to show that the external error is considerably larger than the internal error. Several authors, being primarily concerned with establishing the mean law, have carried only one error, and consequently have been unable to comment on variations.

(ii) In deriving extinction curves, deviating stars have tended to be omitted. This has usually happened following the deliberate exclusion of peculiar or emission line stars, where the assumption has been made that a closer examination of any deviating star will reveal the star or its environment to be peculiar.

(iii) The linear correlations that appear in the $E(\lambda-V)$ versus $E(B-V)$ diagrams [see Fig. 6(d),

© Royal Astronomical Society • Provided by the NASA Astrophysics Data System

1986MNRAS.219..903C

(e) and (f)] have also tended to obscure variations. A fixed law leads to such linear correlations and the immediate conclusion from these diagrams is that the extinction law is fixed. Changes in the values of $A(\lambda)/E(B-V)$ lead to equivalent changes in the slope of these diagrams. A 1 mag change in $A(\lambda)/E(B-V)$ (e.g. from 1 to 2) results in a clearly noticeable 18° change in the slope, whereas a change from 5 to 6 results in a mere 2° change, easily missed by the human eye.

(iv) Most ultraviolet measurements have been provided by satellite experiments for which a calibration has been needed before integrating with ground-based data. Consequently several extinction studies have used only the ultraviolet data and used two ultraviolet wavelengths as the normalization points. Any variations in the ultraviolet extinction near these points is clearly no longer detectable.

(v) The variations found in this paper show that there are relatively small changes in the extinction values between 2200 and 2740 Å. Hence, searches for variations longwards of 2200 Å will probably not show any significant results.

(vi) The $E(\lambda-V)$ versus $E(B-V)$ diagrams show the behaviour of the extinction at wavelength λ. As a point does not have any shape they can obviously not be used for examining changes in the shape of the extinction curve. Instead it is necessary to adopt a different approach such as the algebraic approximation of a straight line plus Lorentzian used in this paper, and look for correlated variations amongst the coefficients.

The large data bank of *IUE* images can also be used to study variations in the extinction law, and many authors have used *IUE* data to look at individual stars (e.g. Massa *et al.* 1983). Three advantages stem from the use of *IUE* data. First, we can increase the wavelength coverage from the 1350–2740 Å of S2/68 to the 1200–3000 Å of *IUE*. Secondly, we can work at the higher resolution of 6A provided by low dispersion *IUE* spectra rather than the 100 Å bands used here, although S2/68 data is available to its resolution limit of 35 Å. Thirdly, the algebraic approximation for the extinction curve can be extended to include a quadratic term:

$$A(\lambda)/E(B-V)=A+B\times x+C\times x^{**}2+G[0.28/)x-4.60)^{**}2+0.28]. \quad (7)$$

This form has been used by Howarth (1983) for the LMC extinction curve and its adoption would allow a study to be made of the far-UV rise which being below 1500 Å is beyond the range of S2/68.

All the extinction curves examined in this paper can be well represented by a straight line plus a Lorentzian. And all the extinction curves seem to be smooth deviations from the mean extinction law, including those for the Magellanic Clouds. There appear to be no extinction curves that are so peculiar that they cannot be reproduced by selecting reasonable values for the scattering slope and 2200 Å feature. So now is perhaps good time for constructing fresh theoretical models to see whether they can throw more light on the interstellar chemistry or the particle size distribution.

11 Conclusions

(i) The interstellar extinction curve is found to vary and at least two agents are required to account for changes in the scattering slope and the strength of the 2200 Å feature.

(ii) The variations are widespread. Significant variations from the mean law (i.e. greater than 1 mag) appear to affect approximately one star in three.

(iii) The variations are smooth. All stars reported as having peculiar extinction are not individually special but merely situated towards the limits of the variations.

(iv) The variations cannot be explained in terms of observational or systematic errors. Photometric errors and spectral misclassification lead to a strong positive correlation between scattering slope and strength of the 2200 Å feature, i.e. steep slopes have strong 2200 Å and

© Royal Astronomical Society • Provided by the NASA Astrophysics Data System

1986MNRAS.219..903C

shallow slopes have weak 2200 Å. Variations in the relative proportions of graphite and silicate lead to a strong negative correlation, i.e. steep slopes have weak 2200 Å and shallow slopes have strong 2200 Å.

(v) No convincing correlations are found between the scattering slope or 2200 Å strength and galactic position or the 4430 Å diffuse feature. This is probably a consequence of the extinction cure being split into components on algebraic rather than physical grounds.

(vi) The profile of the 2200 Å feature is symmetrical and consistent with a Lorentzian centred on 2198 Å, full-half-width 460 Å.

References

Bless, R. C. & Savage, B. D., 1972. *Astrophys. J.,* **171,** 293.
Bohlin, R. C. & Savage, B. S., 1981. *Astrophys. J.,* **249,** 109.
Bromage, G. E. & Nandy, K., 1983. *Mon. Not. R. astr. Soc.,* **204,** 29P.
Carnochan, D. J., 1982. *Mon. Not. R. astr. Soc.,* **201,** 1139.
Draine, B. T. & Lee, H. M., 1984. *Astrophys. J.,* **285,** 89.
Howarth, I. D., 1983. *Mon. Not. R. astr. Soc.,* **203,** 301.
Massa, D. Savage, B. D. & Fitzpatrick, E. L., 1983. *Astrophys. J.,* **266,** 662.
Mathis, J. S., Rumpl, W. & Nordsieck, K. H., 1977. *Astrophys. J.,* **217,** 425.
Meyer, D. M. & Savage, B. D., 1981. *Astrophys. J.,* **248,** 545.
Morales, C., Llorente de Andres, F. & Ruiz del Arbol, J. A., 1980. *Astr. Astrophys.,* **85,** 302.
Nandy, K., Thompson, G. I., Jamar, C., Monfils, A. & Wilson, R., 1975. *Astr. Astrophys.,* **55,** 195.
Nandy, K., Thompson, G. I., Jamar, C., Monfils, A. & Wilson, R., 1976. *Astr. Astrophys.,* **51,** 63.
Nandy, K., Morgan, D. H., Willis, A. J., Wilson, R. & Gondhalekar, P. M., 1981. *Mon. Not. R. astr. Soc.,* **196,** 955.
Savage, B. D., 1975. *Astrophys. J.,* **199,** 92.
Savage, B. D., Wesselius, P. R., Swings, J. P. & The, P. S., 1978. *Astrophys. J.,* **224,** 149.
Seab, C. G., Snow, T. P. & Joseph, C. L., 1980. *Astrophys. J.,* **246,** 788.
Seaton, M. J., 1979. *Mon. Not. R. astr. Soc.,* **187,** 73P.
Snow, T. P. & Seab, C. G., 1980. *Astrophys. J.,* **242,** L83.
Snow, T. P., York, D. G. & Welty, D. E., 1977. *Astr. J.,* **82,** 113.
Willis, A. J. & Wilson, R., 1975. *Astr. Astrophys.,* **44,** 205.
Willis, A. J. & Wilson, R., 1977. *Astr. Astrophys.,* **59,** 133.
Witt, A. N., Bohlin, R. C. & Stecher, T. P., 1984. *Astrophys. J.,* **279,** 698.

© Royal Astronomical Society • Provided by the NASA Astrophysics Data System